Fast Passivity Enforcement of S-Parameter Macromodels by Pole Perturbation

Dirk Deschrijver and Tom Dhaene, *Senior Member, IEEE*

***Abstract*—This paper presents a fast iterative algorithm for passivity enforcement of large nonpassive macromodels that share a common set of poles. It is ensured that the maximum passivity violation is monotonically decreasing in each iteration step, and convergence to a passive macromodel is guaranteed.**

***Index Terms*—Broadband macromodeling, numerical techniques, passivity enforcement, vector fitting.**

I. Introduction

THE SYNTHESIS of accurate broadband macromodels from tabulated S-parameter data is very important for the design of passive microwave systems and devices. Although standard identification techniques are available to extract the model coefficients with a high accuracy, the resulting macromodel is stable, but possibly nonpassive [1]–[3]. Nevertheless, passivity of the macromodel is of crucial importance since a nonpassive model may lead to unstable transient simulations in an unpredictable manner. Several techniques have been considered to address this issue, ranging from convex optimization [4] to Nevanlinna-pick interpolation [5], semidefinite programming [6], linear or quadratic programming [7], residue perturbation [8]–[10], pole perturbation [11], modal perturbation [12], waveform shaping [13], and others [14]–[17].

This paper introduces a new iterative algorithm that is able to enforce passivity by means of a fast pole perturbation scheme. By perturbing only the poles of the macromodel, it is possible to deal with large multiport systems that share a common set of poles in a very efficient way. Although the idea of pole perturbation has been considered before [11], the proposed method is substantially different. This approach perturbs the poles of the model while preserving the zeros, whereas [11] perturbs the poles of the model while preserving the residues. By considering the pole-zero form instead of the pole-residue form, it is possible to derive some analytic conditions which guarantee that the maximum passivity violation is monotonically decreasing in each iteration step. Therefore, it is also guaranteed that the proposed method will converge to a passive macromodel, as illustrated by three examples.

Manuscript received July 18, 2008; revised December 05, 2008. First published February 10, 2009; current version published March 11, 2009. This work was supported by the Fund for Scientific Research Flanders (FWO Vlaanderen).

The authors are with the Department of Information Technology, Ghent University—Institute of Broadband Technology (IBBT), 9000 Ghent, Belgium (e-mail: dirk.deschrijver; tom.dhaene@intec.ugent.be).

Color versions of one or more of the figures in this paper are available online at http://ieeexplore.ieee.org.

Digital Object Identifier 10.1109/TMTT.2009.2013309

II. Passivity Condition

The proposed method in this paper considers a stable, but potentially nonpassive multiport system in state-space form

$$j\omega X(j\omega) = AX(j\omega) + BU(j\omega) \tag{1}$$

$$Y(j\omega) = CX(j\omega) + DU(j\omega) \tag{2}$$

provided that A is the state matrix, B is the input matrix, C is the output matrix, and D is the feedthrough matrix with appropriate dimensions [18] . A stable realization can be obtained by applying the fast vector fitting procedure to some tabulated S-parameter data, while enforcing a common pole set for each matrix element [19]. The associated transfer matrix $H(j\omega)$ is

$$H(j\omega) = C(j\omega I - A)^{-1}B + D. \tag{3}$$

In the case of scattering parameters, the exact definition of passivity stipulates that $H(j\omega)$ must be unitary bounded

$$I - H^*(j\omega)H(j\omega) \geq 0 \qquad \forall\omega \tag{4}$$

such that the following equivalent condition is satisfied:

$$\max_{\omega}(\sigma(j\omega)) \leq 1 \qquad \forall\sigma(H(j\omega)). \tag{5}$$

The singular values curves $\sigma(H(j\omega))$ are then defined as

$$\sigma(H(j\omega)) = \sqrt{\text{eig}(H^*(j\omega)H(j\omega))}. \tag{6}$$

III. Analytic Passivity Test

The passivity of the state-space model can easily be verified by computing the eigenvalues of a Hamiltonian matrix M [21]

$$M = \begin{bmatrix} A - BR^{-1}D^TC & -BR^{-1}B^T \\ C^TQ^{-1}C & -A^T + C^TDR^{-1}B^T \end{bmatrix} \tag{7}$$

where $R = D^TD - I$ and $Q = DD^T - I$. If $j\omega_k$ is an imaginary eigenvalue of the matrix M, then the corresponding frequency ω_k may denote the crossover between a passive and a nonpassive frequency band [20]. By computing the slopes of the singular value curves at the purely imaginary eigenvalues, it is possible to determine the exact boundaries of a passivity violation. If all the eigenvalues of the Hamiltonian matrix M have a nonvanishing real part, then the system is passive [21].

IV. Perturbation Constraints

If the macromodel is nonpassive, then the passivity enforcement algorithm perturbs the common poles of the state-space model until all singular value curves (5) are unitary bounded. During this process, it is ensured that the perturbation does not introduce new violations, which may result at other frequencies. Therefore, some additional constraints must be imposed, which guarantee that the size of the largest passivity violation decreases monotonically in each iteration step. Two specific cases are distinguished: the perturbation of a real pole and the perturbation of a complex conjugate pair of poles.

A. Constraints on a Real Pole

In the case of a real pole perturbation, the perturbed transfer matrix $\tilde{H}(j\omega)$ is obtained by multiplying each matrix element of $H(j\omega)$ by a frequency-dependent factor $\alpha_r(j\omega)$. This factor cancels out the original real pole a_p and introduces a perturbed real pole $\tilde{a}_p$, which yields a modified transfer function

$$\tilde{H}(j\omega) = H(j\omega)\alpha_r(jw) = H(j\omega)\frac{(j\omega - a_p)}{(j\omega - \tilde{a}_p)}. \quad (8)$$

The singular values of $\tilde{H}(j\omega)$ are then described as follows:

$$\sigma(\tilde{H}(j\omega)) = \sqrt{\mathrm{eig}(\alpha_r^*(j\omega)H^*(j\omega)H(j\omega)\alpha_r(j\omega))} \quad (9)$$
$$= |\alpha_r(j\omega)|\sigma(H(j\omega)). \quad (10)$$

To ensure that the compensation does not introduce new violations elsewhere, $|\alpha_r(j\omega)| \leq 1$ must hold for *all* ω, hence,

$$\left|\frac{j\omega - a_p}{j\omega - \tilde{a}_p}\right| \leq 1 \Leftrightarrow |j\omega - a_p|^2 \leq |j\omega - \tilde{a}_p|^2 \qquad \forall\omega \in \Re. \quad (11)$$

Since $\tilde{a}_p$ must be stable, it follows that $\Re e(\tilde{a}_p) \leq \Re e(a_p)$.

B. Constraints on a Complex Pole Pair

In the case of a complex pole perturbation, the perturbed transfer matrix $\tilde{H}(j\omega)$ is obtained by multiplying each matrix element of $H(j\omega)$ by a frequency-dependent factor $\alpha_c(j\omega)$. This factor cancels out the original complex conjugate poles a_p, a_p^* and introduces a perturbed set of complex conjugate poles $\tilde{a}_p, \tilde{a}_p^*$, which yields a modified transfer function

$$\tilde{H}(j\omega) = H(j\omega)\alpha_c(jw) = H(j\omega)\frac{(j\omega - a_p)(j\omega - a_p^*)}{(j\omega - \tilde{a}_p)(j\omega - \tilde{a}_p^*)}. \quad (12)$$

The effect on the singular values of $\tilde{H}(j\omega)$ is similar

$$\sigma(\tilde{H}(j\omega)) = \sqrt{\mathrm{eig}(\alpha_c(j\omega)^* H(j\omega)^* H(j\omega)\alpha_c(j\omega))} \quad (13)$$
$$= |\alpha_c(j\omega)|\,\sigma(H(j\omega)). \quad (14)$$

To ensure that the compensation does not introduce new violations elsewhere, $|\alpha_c(j\omega)| \leq 1$ must hold for *all* ω, hence,

$$\left|\frac{(j\omega - a_p)(j\omega - a_p^*)}{(j\omega - \tilde{a}_p)(j\omega - \tilde{a}_p^*)}\right| \leq 1 \qquad \forall\omega \in \Re \quad (15)$$
$$\Leftrightarrow \left|(j\omega - \tilde{a}_p)(j\omega - \tilde{a}_p^*)\right|^2 - \left|(j\omega - a_p)(j\omega - a_p^*)\right|^2 \geq 0 \qquad \forall\omega \in \Re \quad (16)$$
$$\Leftrightarrow \omega^2(-2\,|\tilde{a}_p|^2 + 4\Re e(\tilde{a}_p)^2 + 2\,|a_p|^2 - 4\Re e(a_p)^2) + |\tilde{a}_p|^4 - |a_p|^4 \geq 0 \qquad \forall\omega \in \Re \quad (17)$$

where the second-order polynomial on the left-hand side is nonnegative for every $\omega \in \Re$ if and only if

$$\Re e(\tilde{a}_p)^2 + \Im m(\tilde{a}_p)^2 \geq \Re e(a_p)^2 + \Im m(a_p)^2 \quad (18)$$

and

$$\Re e(\tilde{a}_p)^2 - \Im m(\tilde{a}_p)^2 \geq \Re e(a_p)^2 - \Im m(a_p)^2 \quad (19)$$

provided that the perturbed complex poles $\tilde{a}_p, \tilde{a}_p^*$ are stable.

C. Visualization of Perturbation Area

The previous conditions allow the algorithm to pinpoint exactly the region in which a perturbed pole can be located without introducing new passivity violations. It suffices to add some attenuation to real poles, but more relaxed conditions are derived for complex conjugate poles (18), (19). In the latter case, the complex pole perturbation area is bounded by the following.

- A circle (18) that is centered at the origin with radius $|a_p|$, having the following parametric coordinates

$$\Re e(\tilde{a}_p) = |a_p|\cos(t) \quad \Im m(\tilde{a}_p) = |a_p|\sin(t). \quad (20)$$

- An orthogonal hyperbola (19) that is centered at the origin with a given parameter $\gamma = \Re e(a_p)^2 - \Im m(a_p)^2$.
  — If $\gamma > 0$, then the hyperbola has an east–west opening

$$\Re e(\tilde{a}_p) = \sqrt{|\gamma|}\sec(t) \quad \Im m(\tilde{a}_p) = \sqrt{|\gamma|}\tan(t). \quad (21)$$

  — If $\gamma < 0$, then the hyperbola has a north–south opening

$$\Re e(\tilde{a}_p) = \sqrt{|\gamma|}\tan(t) \quad \Im m(\tilde{a}_p) = \sqrt{|\gamma|}\sec(t). \quad (22)$$

  — If $\gamma = 0$, then the hyperbola reduces to the asymptotes.

A visual illustration of the circle and hyperbola is shown in Fig. 1 ($\gamma > 0$), Fig. 2 ($\gamma < 0$), and Fig. 3 ($\gamma = 0$), where the valid pole perturbation area is marked in grey.

V. Perturbation Algorithm

This section presents a simple, but efficient scheme that removes passivity violations by perturbing the poles of the macromodel. First, the Hamiltonian passivity check (as described in Section III) is used to determine the passivity of the macromodel. If the macromodel is found to be nonpassive, then an iterative algorithm is applied, which consists of the following steps.

Step 1) Find the frequency ω_{viol} that corresponds to the largest passivity violation based on the eigenvalues of (7).

Step 2) Select the pole a_p of the model for which the contribution to the largest passivity violation $\Delta H_p(\omega_{\mathrm{viol}})$ is maximal.

Step 3) Perturb the pole such that the passivity violation becomes smaller, without introducing new violations. At the same time, minimize the model deviation by error control.

These steps are repeated iteratively until the macromodel is assumed passive. As a final step, the passivity is verified by recomputing the eigenvalues of a Hamiltonian matrix.

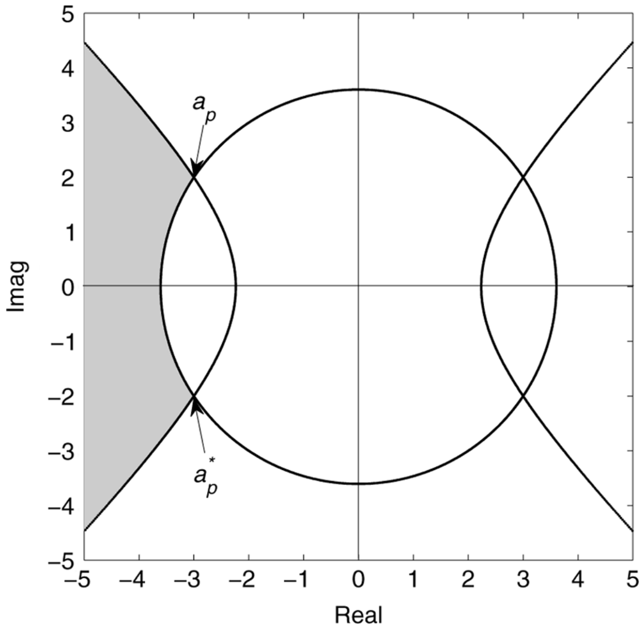

Fig. 1. Pole perturbation area for $\{a_p, a_p^*\} = -3 \pm 2j(\gamma > 0)$.

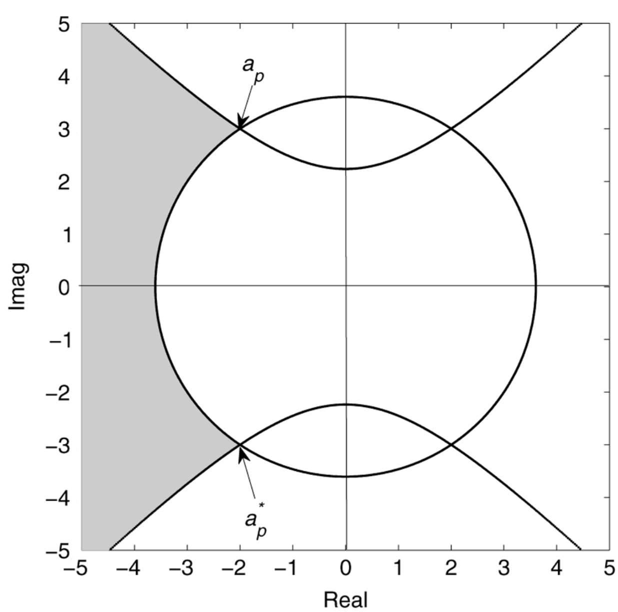

Fig. 2. Pole perturbation area for $\{a_p, a_p^*\} = -2 \pm 3j(\gamma < 0)$.

A. *Selection of the Relevant Pole*

As mentioned in Section III, it is possible to exactly pinpoint the nonpassive regions of the spectrum by considering the purely imaginary eigenvalues of the Hamiltonian matrix (7). A simple optimization algorithm can then be applied to find the frequency ω_{viol}, which corresponds to the largest passivity violation. This problem converges fast since the optimization involves only one variable and the midpoints of each interval can be used as a good initial guess. Details about this procedure are well described in the literature (see [8] and [22]).

For each pole a_p of the macromodel, the contribution $\Delta H_p(\omega_{\mathrm{viol}})$ to the largest passivity violation can be computed

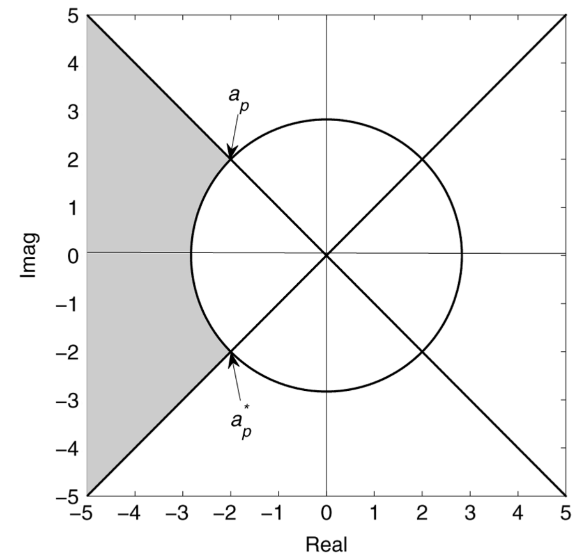

Fig. 3. Pole perturbation area for $\{a_p, a_p^*\} = -2 \pm 2j(\gamma = 0)$.

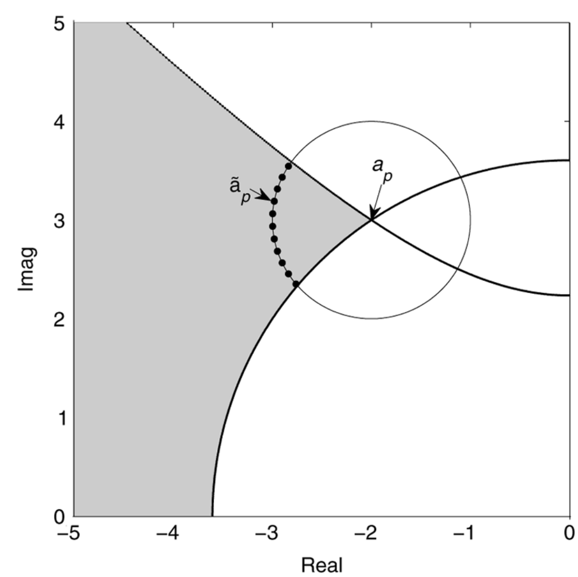

Fig. 4. Second quadrant of Fig. 2: dots represent valid candidate poles.

as the L_2-norm of the corresponding residue matrix fraction

$$\Delta H_p(\omega_{\mathrm{viol}}) = \left\| \frac{C_p}{j\omega_{\mathrm{viol}} - a_p} \right\|_2, \qquad \text{for } p = 1, \ldots, P. \quad (23)$$

The pole a_p that corresponds to the largest contribution $\Delta H_p(\omega_{\mathrm{viol}})$ is perturbed to compensate the passivity violation.

B. *Perturbation of the Pole*

If a_p is a real pole, then it suffices to add some attenuation such that $\tilde{a}_p = r a_p$, where $r > 1$ is a positive real parameter.

If a_p is a complex pole, then a circle is formed, which is centered at the pole a_p, having a small positive radius $r > 0$

$$(x - \Re e(a_p))^2 + (y - \Im m(a_p))^2 = r^2. \quad (24)$$

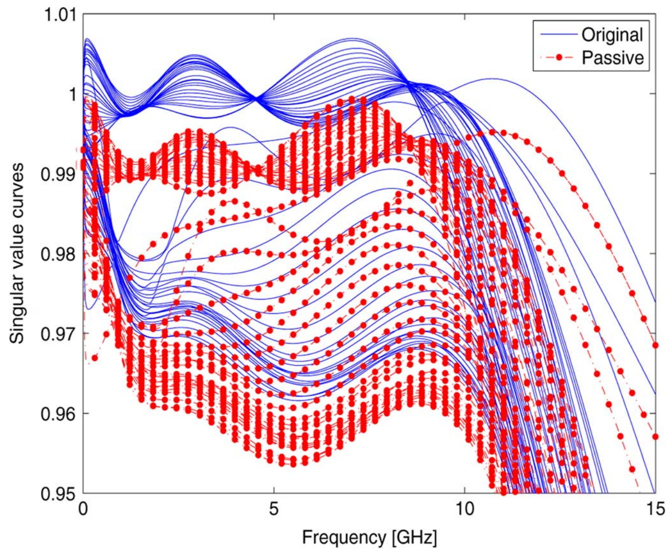

Fig. 5. BGA package: singular values of scattering matrix.

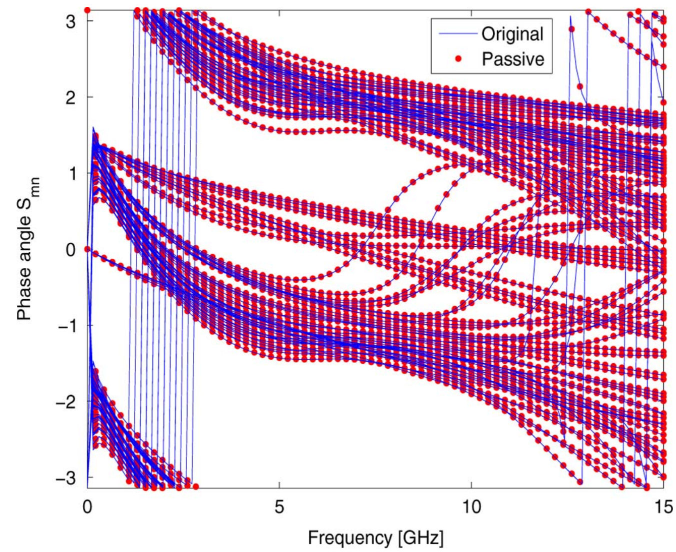

Fig. 7. BGA package: phase angle of matrix elements (subset).

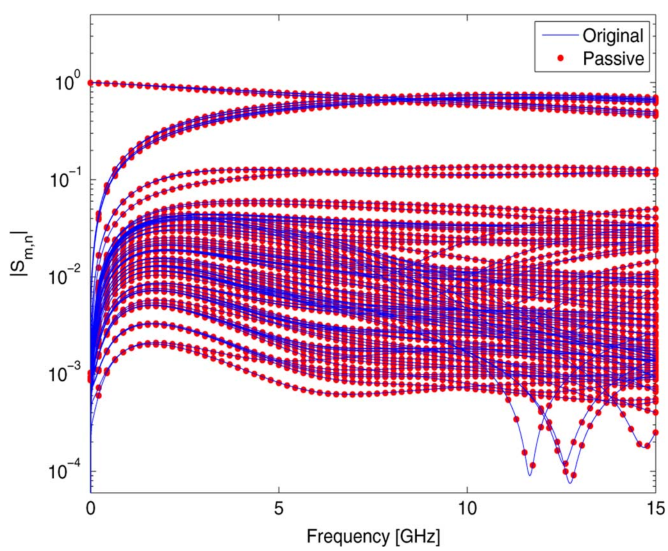

Fig. 6. BGA package: magnitude of matrix elements (subset).

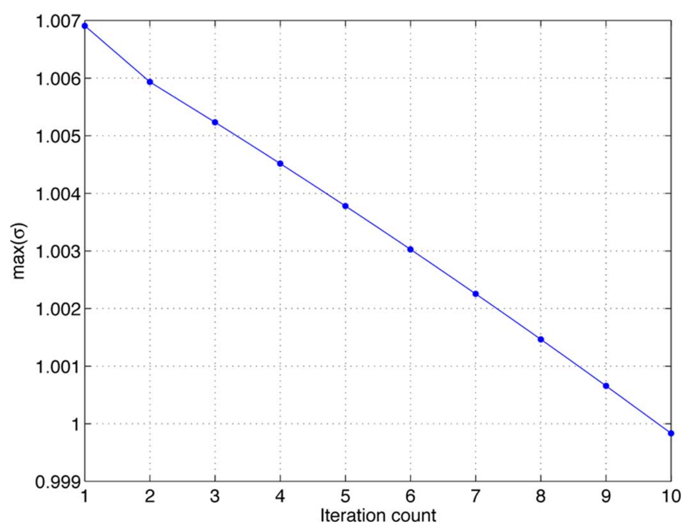

Fig. 8. BGA package: maximum singular value in each iteration step.

Some tuples (x_k, y_k), which are equidistantly spread over the circle (24), are chosen to form complex conjugate pairs of candidate poles $\tilde{a}_{p,k} = x_k + jy_k$ and $\tilde{a}^*_{p,k} = x_k - jy_k$. Only the valid pole pairs, which satisfy the perturbation constraints (18) and (19), are retained. For each of the remaining pole pairs, the algorithm computes the least squares error $||\tilde{H}(j\omega) - H(j\omega)||_2$ that would be introduced over the frequency range of interest if the original poles are replaced by the candidate poles [see (12)]. The pole pair that corresponds to the smallest error is then effectively used for the replacement. A visual illustration is shown in Fig. 4 in case $\gamma < 0$. Although a minimization of the least squares fitting error is suggested in this paper, it is clear that any kind of error criterion (absolute or relative) can be used instead [11], [23].

C. Iteration Scheme

This perturbation process is repeated iteratively until all passivity violations are removed. Since the perturbation of the poles guarantees that no new passivity violations are introduced in each iteration step, it suffices to compute the eigenvalues of the Hamiltonian matrix only once at the beginning and once at the end of the algorithm. It is noted that the convergence speed of the iteration scheme depends on the value of r that is chosen in Section V-B. In practice, it can be chosen in such a way that the pole perturbation factor $|\alpha_r(j\omega)|$ and $|\alpha_c(j\omega)|$ in (10) or (14) compensates approximately a certain percentage of the largest passivity violation in each iteration step. The percentage is a tuning parameter that allows the designer to find an acceptable tradeoff between efficiency (a few large compensations) and accuracy (several small compensations).

VI. Example: 48-Port Ball Grid Array (BGA) Package

In this example, the presented approach is used to compute a passive macromodel of a 48-port BGA package [11]. The scattering parameters of the structure are simulated with Agilent EEsof Momentum [24] from dc up to 10 GHz, and vector fitting is used to approximate the response by a six-pole proper transfer function using 100 data samples [7]. It is seen from Fig. 5 that the macromodel has several nonnegligle passivity

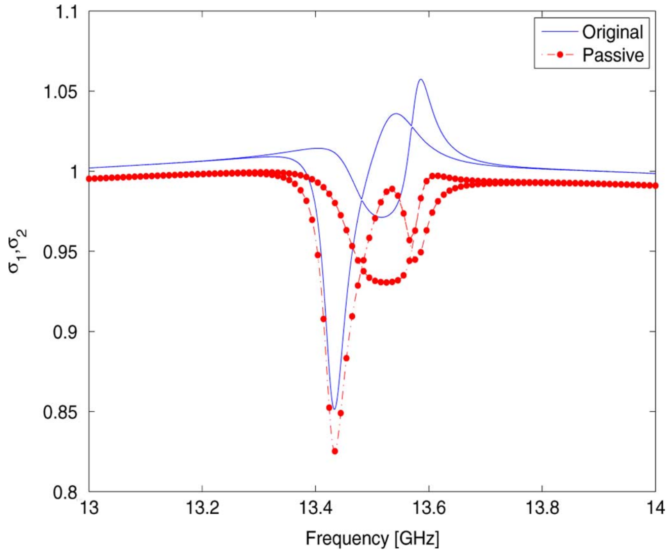

Fig. 9. Hairpin filter: singular values of scattering matrix.

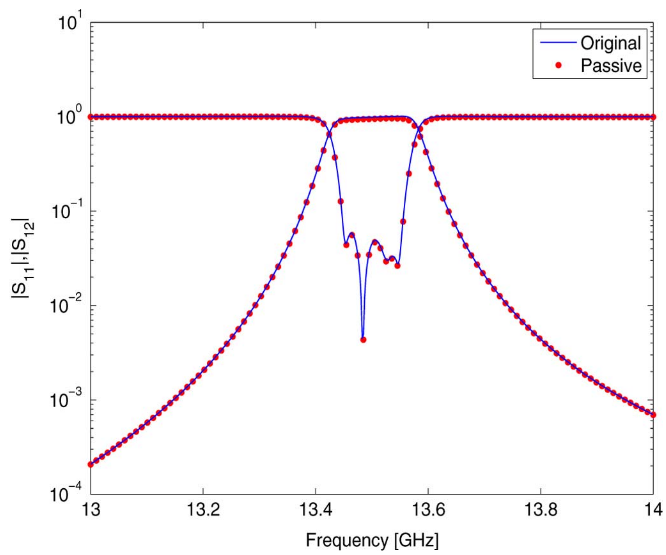

Fig. 10. Hairpin filter: magnitude of matrix elements.

violations both inside and outside the frequency range of interest. The proposed passivity enforcement procedure is applied to compensate the violations, and converges to a passive macromodel in only 18 s on a Dual Core 2.4-GHz laptop computer. Figs. 6 and 7 show that the accuracy of the overall macromodel is well preserved, both in terms of the magnitude and the phase angle, respectively. The worst case error over all matrix elements is −43 dB, which is quite small given the size of the maximum violation ($\sigma_{\max} = 1.0069$). The rms deviation that was introduced by the perturbations corresponds to 3×10^{-2}. It is seen from Fig. 8 that the maximum singular value of the scattering matrix decreases monotonically in each iteration step. The algorithm converges in ten iterations to a guaranteed passive macromodel.

VII. Example: Two-Port Hairpin Filter

In this example, the presented approach is used to compute a passive macromodel of a two-port microwave hairpin filter [11].

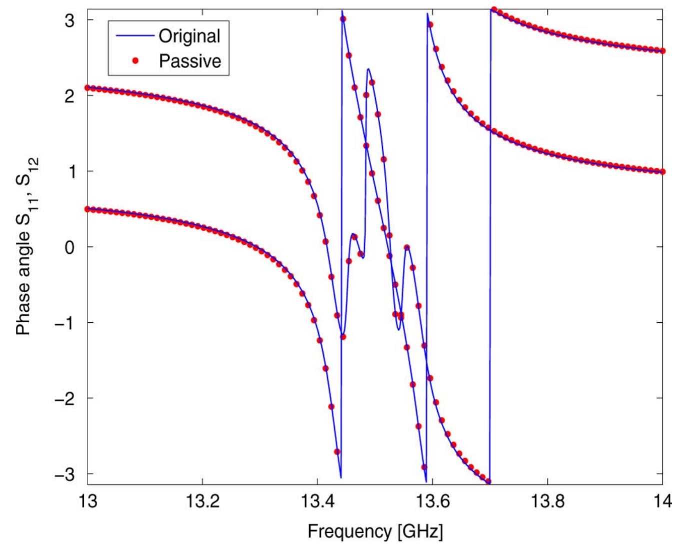

Fig. 11. Hairpin filter: phase angle of matrix elements.

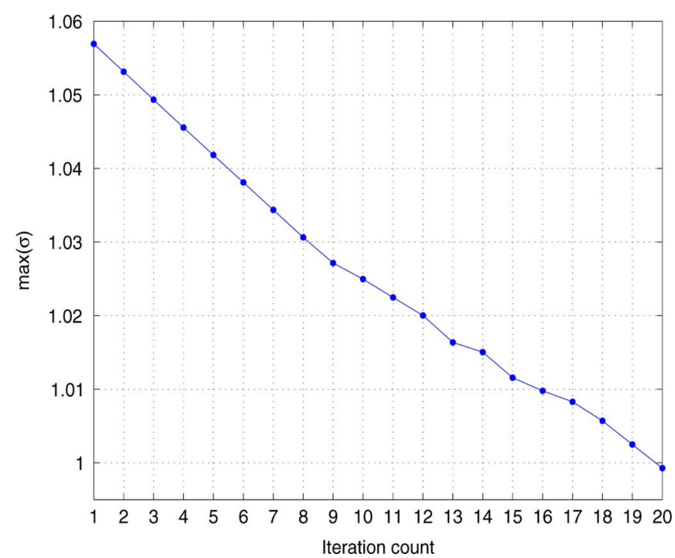

Fig. 12. Hairpin filter: maximum singular value in each iteration step.

The scattering parameters of the structure are simulated in the frequency domain and vector fitting is used to approximate the frequency response by a ten-pole proper transfer function [7]. It is seen from Fig. 9 that the macromodel has some in-band passivity violations at the higher frequencies. The passivity enforcement procedure is applied to compensate them, and converges to a passive macromodel in only 2.8 s on the same laptop computer. Figs. 10 and 11 show that the accuracy of the overall macromodel is again well preserved, both in terms of the magnitude and the phase angle respectively. The rms deviation that was introduced by the algorithm from dc up to 15 GHz corresponds to 8×10^{-3}, which is acceptable. As can be seen from Fig. 12, the maximum singular value of the scattering matrix decreases monotonically in each iteration step, and the algorithm converges in 20 iterations to a guaranteed overall passive macromodel.

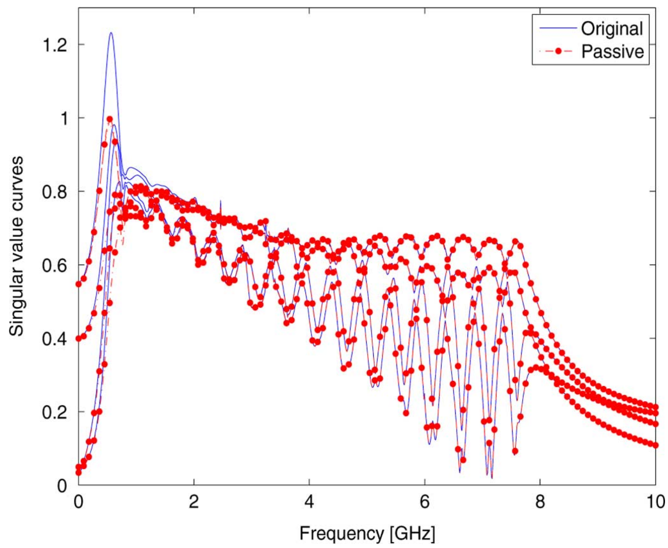

Fig. 13. Interconnect: singular values of scattering matrix.

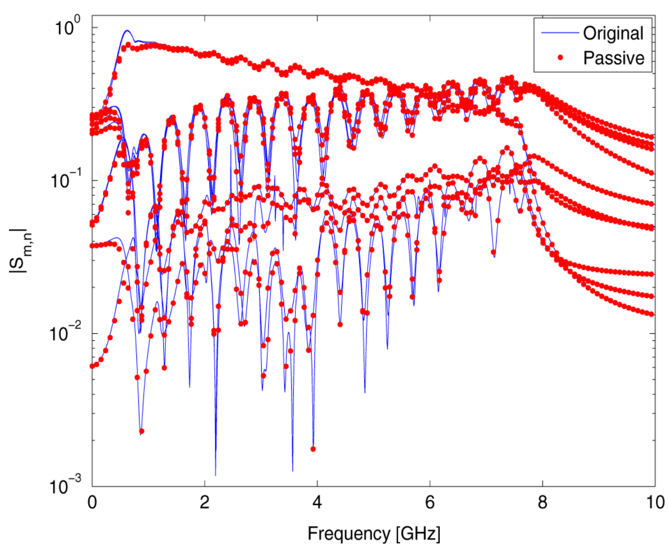

Fig. 14. Interconnect: magnitude of matrix elements.

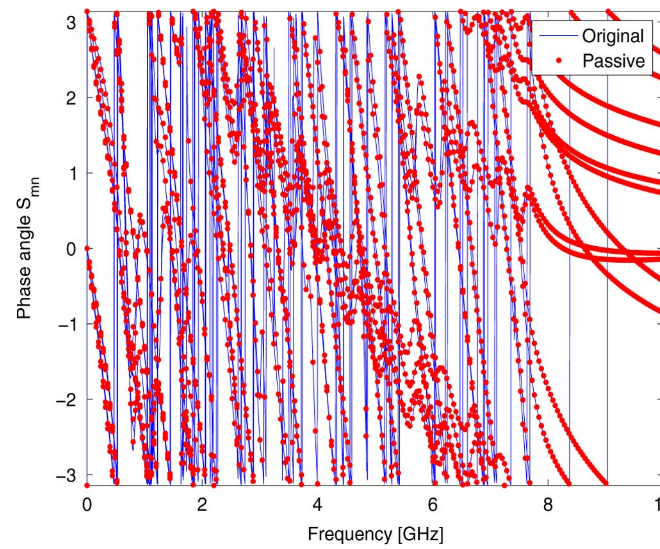

Fig. 15. Interconnect: phase angle of matrix elements.

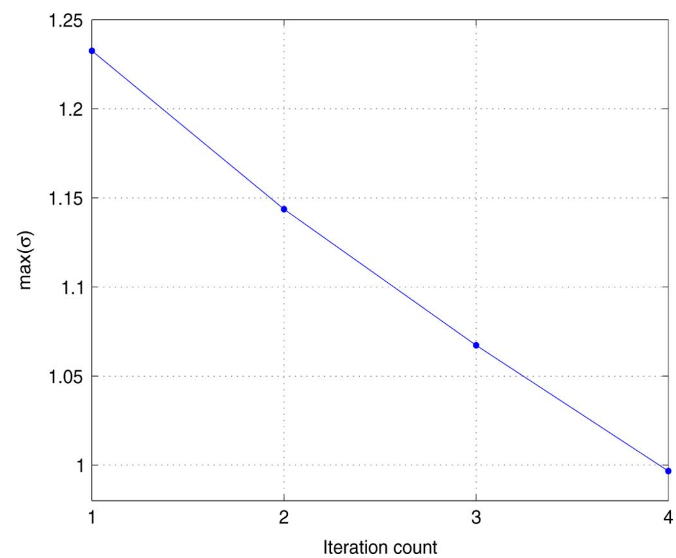

Fig. 16. Interconnect: maximum singular value in each iteration step.

VIII. Example: Four-Port Interconnect

In this example, the presented approach is used to compute a passive macromodel of a four-port interconnect system [25]. The scattering parameters of the structure are measured in the frequency domain from 0.775 to 7.52 GHz and vector fitting is used to approximate the response by a 100-pole proper transfer function [7]. It is seen from Fig. 13 that the macromodel has quite a large outband passivity violation at the lower frequencies. The passivity enforcement procedure is applied to compensate them, and converges to a passive macromodel in only 1.8 s. The rms deviation between the original and the passive model is 3×10^{-2}. Due to the size of the passivity violation, some visible difference can be distinguished between the frequency response of both models in the vicinity of the violation, as shown in Figs. 14 and 15. It is clear from Fig. 16 that the maximum singular value of the scattering matrix decreases monotonically in each iteration step, and that the algorithm converges in four iterations to a guaranteed passive macromodel.

IX. Conclusion

This paper has presented an iterative algorithm for passivity enforcement of large state space macromodels, which are based on a common pole set. The maximum singular value of the scattering matrix decreased monotonically in each iteration step, and convergence to a passive macromodel is guaranteed. Three examples have illustrated the efficiency of the approach.

Acknowledgment

The authors would like to thank Dr. A. Lamecki and Dr. W. Beyene for providing the data sets in [11] and [25], and Dr. B. Gustavsen for providing the nonpassive rational macromodels in [7].

References

[1] B. Gustavsen and A. Semlyen, “Rational approximation of frequency domain responses by vector fitting,” *IEEE Trans. Power Del.*, vol. 14, no. 3, pp. 1052–1061, Jul. 1999.

[2] D. Deschrijver, B. Haegeman, and T. Dhaene, "Orthonormal vector fitting: A robust macromodeling tool for rational approximation of frequency domain responses," *IEEE Trans. Adv. Packag.*, vol. 30, no. 2, pp. 216–225, May 2007.

[3] D. Deschrijver, B. Gustavsen, and T. Dhaene, "Advancements in iterative methods for rational approximation in the frequency domain," *IEEE Trans. Power Del.*, vol. 22, no. 3, pp. 1633–1642, Jul. 2007.

[4] C. P. Coelho, J. R. Phillips, and L. M. Silveira, "A convex programming approach for generating guaranteed passive approximations to tabulated frequency-data," *IEEE Trans. Comput.-Aided Design Integr. Circuits Syst.*, vol. 23, no. 2, pp. 293–301, Feb. 2004.

[5] C. P. Coelho, L. M. Silveira, and J. R. Phillips, "Passive constrained rational approximation algorithm using Nevanlinna-pick interpolation," in *Design Automat. Test in Eur. Conf. Exhibition*, Mar. 2002, pp. 923–930.

[6] H. Chen and J. Fang, "Enforcing bounded realness of S-parameter through trace parameterization," in *IEEE Elect. Perform. Electron. Packag. Conf.*, Oct. 2003, pp. 291–294.

[7] B. Gustavsen, "Fast passivity enforcement for S-parameter models by perturbation of residue matrix eigenvalues," *IEEE Trans. Adv. Packag.*, 2009, accepted for publication.

[8] S. Grivet-Talocia, "Passivity enforcement via perturbation of hamiltonian matrices," *IEEE Trans. Power Del.*, vol. 51, no. 9, pp. 1755–1769, Sep. 2004.

[9] D. Saraswat, R. Achar, and M. S. Nakhla, "Fast passivity verification and enforcement via reciprocal systems for interconnects with large order macromodels," *IEEE Trans. Very Large Scale Integr. (VLSI) Syst.*, vol. 15, no. 1, pp. 48–59, Jan. 2007.

[10] T. Dhaene, D. Deschrijver, and N. Stevens, "Efficient algorithm for passivity enforcement of S-parameter based macromodels," *IEEE Trans. Microw. Theory Tech.*, vol. 57, no. 2, pp. 415–420, Feb. 2009.

[11] A. Lamecki and M. Mrozowski, "Equivalent SPICE circuits with guaranteed passivity from nonpassive models," *IEEE Trans. Microw. Theory Tech.*, vol. 55, no. 3, pp. 526–532, Mar. 2007.

[12] B. Gustavsen, "Passivity enforcement of rational models via modal perturbation," *IEEE Trans. Power Del.*, vol. 23, no. 2, pp. 768–775, Apr. 2008.

[13] B. Yan, P. Liu, S. X. Tan, and B. McGaughy, "Passive modeling of interconnects by waveform shaping," in *8th Int. Quality Electron. Design Symp.*, Mar. 2007, pp. 356–361.

[14] R. Gao, Y. S. Mekonnen, W. T. Beyene, and J. E. Schutt-Aine, "Black-box modeling of passive systems by rational function approximation," *IEEE Trans. Adv. Packag.*, vol. 28, no. 2, pp. 209–215, May 2005.

[15] S. H. Min and M. Swaminathan, "Construction of broadband passive macromodels from frequency data for simulation of distributed interconnect networks," *IEEE Trans. Electromagn. Compat.*, vol. 46, no. 4, pp. 544–558, Nov. 2004.

[16] T. D'Haene and R. Pintelon, "Passivity enforcement of transfer functions," *IEEE Trans. Instrum. Meas.*, vol. 57, no. 10, pp. 2181–2187, Oct. 2008.

[17] A. Chinea and S. Grivet-Talocia, "Perturbation schemes for passivity enforcement of delay-based transmission line macromodels," *IEEE Trans. Adv. Packag.*, vol. 31, no. 3, pp. 568–578, Aug. 2008.

[18] J. S. Bay, *Fundamentals of Linear State Space Systems*, 1st ed. New York: McGraw-Hill, 1998.

[19] D. Deschrijver, M. Mrozowski, T. Dhaene, and D. De Zutter, "Macromodeling of multiport systems using a fast implementation of the vector fitting method," *IEEE Microw. Wireless Compon. Lett.*, vol. 18, no. 6, pp. 383–385, Jun. 2008.

[20] S. Boyd, L. El Ghaoui, E. Feron, and V. Balakrishnan, *Linear Matrix Inequalities in System and Control Theory*. Philadelphia, PA: SIAM, 1994.

[21] S. Boyd, V. Balakrishnan, and P. Kabamba, "A bisection method for computing the H_∞ norm of a transfer matrix and related problems," *Math. Control, Signals, Syst.*, vol. 2, pp. 207–219, 1989.

[22] D. Saraswat, R. Achar, and M. Nakhla, "Enforcing passivity for rational function based macromodels of tabulated data," in *IEEE Elect. Perform. Electron. Packag. Conf.*, Oct. 2003, pp. 295–298.

[23] S. Grivet-Talocia and A. Ubolli, "Passivity enforcement with relative error control," *IEEE Trans. Microw. Theory Tech.*, vol. 55, no. 11, pp. 2374–2383, Nov. 2007.

[24] Agilent EEsof Comms EDA, ADS Momentum Softw. Agilent Technol., Santa Rosa, CA, 2006.

[25] W. T. Beyene, J. Feng, N. Cheng, and X. Yuan, "Performance analysis and model-to-hardware correlation of multigigahertz parallel bus with transmit pre-emphasis equalization," *IEEE Trans. Microw. Theory Tech.*, vol. 53, no. 11, pp. 3568–3577, Nov. 2005.

Dirk Deschrijver was born in Tielt, Belgium, on September 26, 1981. He received the Master degree (Licentiaat) in computer science and Ph.D. degree from the University of Antwerp, Antwerp, Belgium, in 2003 and 2007, respectively.

He was with the Computer Modeling and Simulation (COMS) Group, University of Antwerp, where he was supported by a research project of the Fund for Scientific Research Flanders (FWOVlaanderen). From May to October 2005, he was a Marie Curie Fellow with the Scientific Computing Group, Eindhoven University of Technology, Eindhoven, The Netherlands. He is currently an FWO Post-Doctoral Research Fellow with the Department of Information Technology (INTEC), Ghent University, Gent, Belgium. His research interests include rational least squares approximation, orthonormal rational functions, system identification, and parametric macromodeling techniques.

Tom Dhaene (M'94–SM'05) was born in Deinze, Belgium, on June 25, 1966. He received the Ph.D. degree in electrotechnical engineering from the University of Ghent, Ghent, Belgium, in 1993.

From 1989 to 1993, he was a Research Assistant with the Department of Information Technology, University of Ghent, where his research focused on different aspects of full-wave electromagnetic (EM) circuit modeling, transient simulation, and time-domain characterization of high-frequency and high-speed interconnections. In 1993, he joined the EDA company Alphabit (now part of Agilent Technologies). He was one of the key developers of the planar EM simulator ADS Momentum, and he is the principal developer of the multivariate EM-based adaptive metamodeling tool ADS Model Composer. He was a Professor with the Computer Modeling and Simulation (COMS) Group, Department of Mathematics and Computer Science, University of Antwerp, Antwerp, Belgium. He is currently a Full Professor with the Department of Information Technology, Ghent University, Ghent, Belgium. He has authored or coauthored over 100 peer-reviewed papers and abstracts in international conference proceedings, journals, and books.